3. Experimental Details

In the course of this work, 2 different THz-transmission spectrometers were built. The "MHz-setup" is driven by 10-fs, 10-nJ pulses at a 75-MHz repetition rate and allows for high-quality measurements of the steady-state THz response of a given sample as well as the instantaneous THz response of a sample that was optically excited by relatively weak pump pulses. In contrast, the "kHz-setup" is driven by optimized 1-mJ pulses at a 1-kHz repetition rate and permits measurements of the instantaneous THz response of strongly excited samples such as laser-generated gas plasmas. In the following, the laser systems and the THz spectrometers together with the work sequence of THz spectroscopy are described.

3.1. Laser Systems

3.1.1. MHz-Laser Oscillator

A laser is a light oscillator consisting of an optical resonator and an amplification unit. The latter coherently amplifies the transmitted light and thus compensates for losses such as light that is coupled out for the user. The amplification mechanism is called "light amplification by stimulated emission of radiation" which also coined the term LASER for such an oscillator.[1]

Ti-doped sapphire, Ti:Al_2O_3, is the perfect amplification material to generate ultrashort laser pulses. Pumping Ti:sapphire with 532-nm light results in an extremely broad emission band ranging from 650 to 850 nm [Hir98]. A linear optical resonator of length l restricts the radiation to longitudinal modes $j \in \mathbb{N}$ with frequency $f_j = j\Delta f$ where $\Delta f = c/2l$. Continuous-wave lasing generally starts at 1 frequency f_{j_0} since the amplification profile of Ti:sapphire is homogeneously broadened.

How can one couple many longitudinal modes coherently to generate pulsed radiation? One way is to modulate some suitable parameter of the laser with frequency Δf which results in spectral sidebands at $f_{j_0} \pm \Delta f$. These sidebands are also amplified and in turn generate sidebands and so on, eventually leading to a large number of phase-locked laser modes.

[1] A. Schawlow, one of the inventors of the laser, once joked that no one wanted to call a laser an oscillator since this would turn the laser into a LOSER [Yen87].

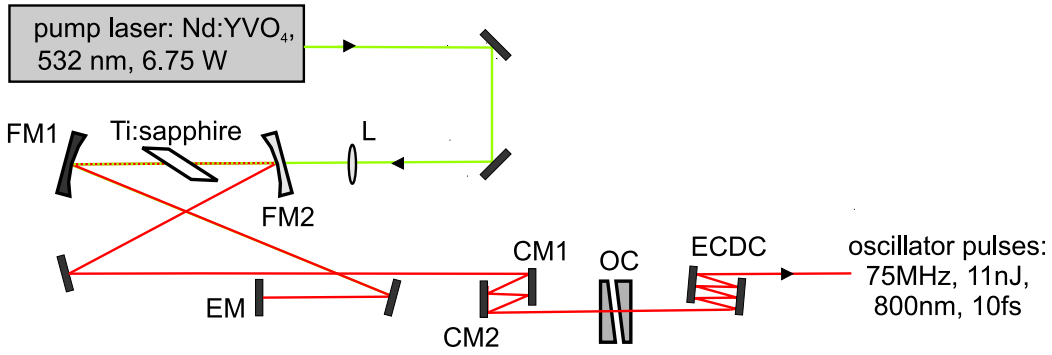

Figure 3.1.: Schematic of the MHz-laser oscillator (Femtosource M1, Femtolasers GmbH). The light-amplifying Ti:sapphire crystal is pumped by a continuous-wave Nd:YVO_4 laser via a focusing lens L. The linear optical resonator is formed by the end mirror EM and the slightly transmitting output coupler OC. The focusing mirrors FM1 and FM2 are responsible for a high power density in the crystal thus enhancing the Kerr effect. Chirped mirrors CM1 and CM2 compensate for the group-velocity dispersion accumulated by 1 pulse roundtrip in the resonator. All beams are incident on the Ti:sapphire crystal under the Brewster angle to minimize losses, and the orientation of FM1 and FM2 is chosen to compensate for the astigmatism introduced by the Ti:sapphire crystal. The OC has the shape of a double-wedge to avoid multiple reflections into and out of the resonator. The external cavity dispersion control ECDC consists of 2 chirped mirrors where each double reflection compensates for the dispersion introduced by a 1-mm thick plate of BK7 glass.

Ti:sapphire permits passive mode locking, that is, self-modulation of the resonator via the optical Kerr-effect. This $\chi^{(3)}$ effect causes a change in the refractive index of the Ti:sapphire crystal which is proportional to the instantaneous light intensity. As a result, the Gaussian intensity profile of the laser beam induces an index profile which acts as a transient lens and so modulates the resonator with the desired frequency Δf provided pulsed operation is on. So-called "chirped mirrors" in the resonator compensate for the group-velocity dispersion of the Ti:sapphire crystal which would increase the duration of the laser pulse and finally switch the Kerr lens off. The use of broadband reflecting and chirped mirrors enables the generation of pulses with a duration of 10 fs and less. Details of the femtosecond laser-oscillator used are shown and described in Fig. 3.1.

3.1.2. kHz-Amplified Laser System

Many optical experiments, for example pump-probe experiments with highly excited samples, require laser-pulse energies much higher than those generated by the MHz oscillator described in the previous section. Larger pulse energies are obtained by amplifying the MHz oscillator pulses in another Ti:sapphire crystal. Since the latter produces a limited output power of $\sim$ 1 W the pulse repetition rate has to be reduced to the kHz range by pulse pickers like a Pockels cell. The so-called seed-laser pulses are temporally stretched before entering the amplification stage in order to avoid too high peak intensities which could induce undesired nonlinear effects in the optical components or even damage them. After several amplification passes, the resulting laser pulses are temporally compressed.

Figure 3.2 shows the kHz amplifier used in this work. In this system, an acousto-optic

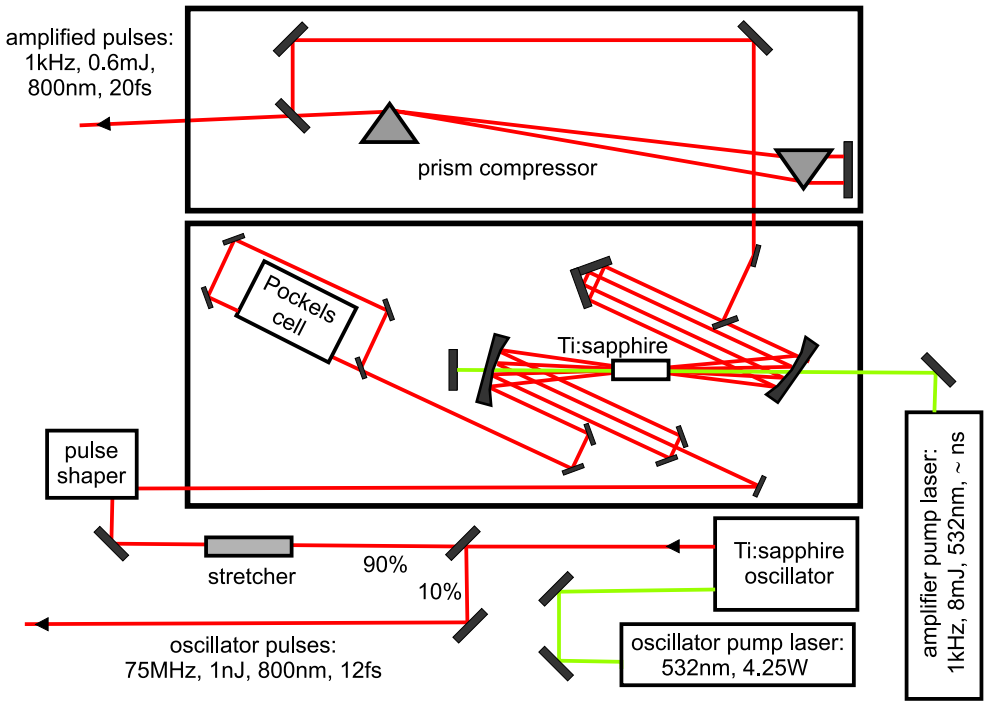

Figure 3.2.: Schematic of the kHz-laser amplifier (Femtopower Compact Pro, Femtolasers GmbH). The seed-laser pulses are produced by a laser oscillator similar to that in Fig. 3.1. Its 75-MHz repetition rate serves as the master clock and is fed into a frequency divider and low-jitter delay generator to provide a synchronized 1 kHz trigger for the pulse shaper, the Pockels cell, and the Nd:YLF-pump laser which pumps another Ti:sapphire crystal with 10-ns pulses. 10 % of the oscillator power is used for other applications whereas the remaining pulses are stretched to a duration of $\approx$ 5 ps and shaped by an acousto-optic programmable dispersive filter (Dazzler, Fastlite). They pass a Ti:sapphire crystal 4 times and subsequently transmit a Pockels-cell pulse picker where the repetition rate is reduced to 1 kHz. After another 5 passes of amplification, the pulses are compressed to a duration of $\approx$ 20 fs by a prism compressor. They have an energy of $\approx$ 0.8 mJ and a center wavelength of 800 nm.

dispersive filter allows for amplitude and phase shaping of the seed pulses to optimize the amplified pulses for the experiment. The frequency divider and delay generator used were developed together with the electronic workshop of the physics department. They generate delays of up to 1 ms with a temporal jitter of less than 100 ps.

3.2. THz Spectrometer

The two THz spectrometers constructed during the work of this thesis are driven by the laser oscillator and the amplified laser system with a 75-MHz an a 1-kHz repetition rate, respectively. The “MHz setup” and the “kHz setup” are based on the same schematic which is shown in Fig. 3.3. However, they differ in some details which will be explained in the following for the various stages of the THz spectrometer.

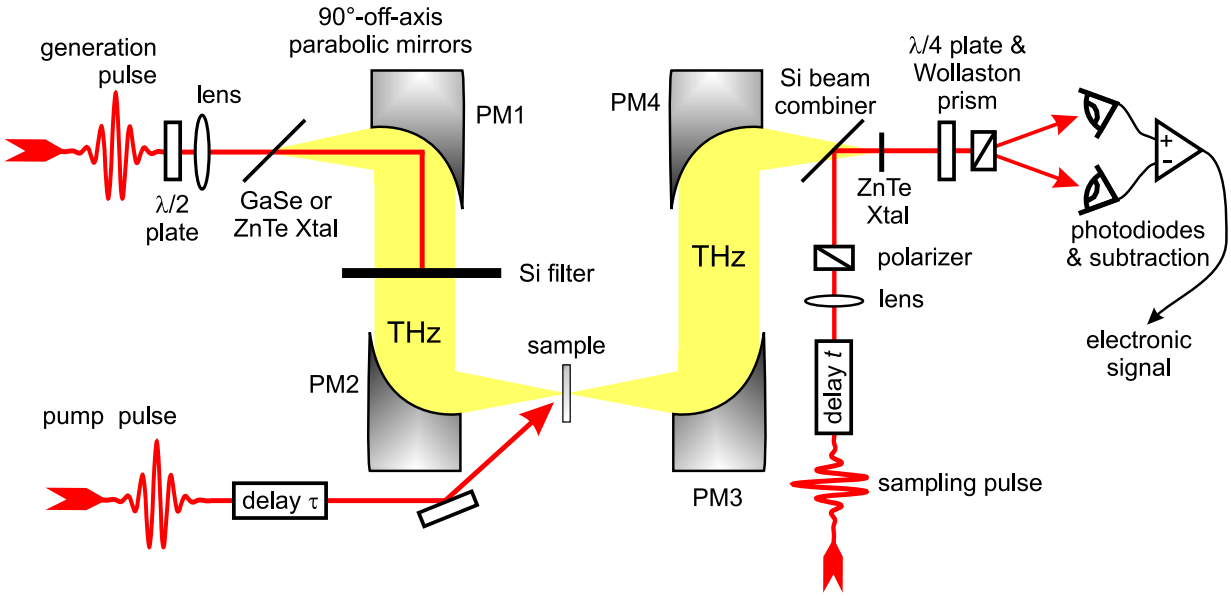

Figure 3.3.: Schematic of the THz spectrometer. A near-infrared generation pulse from a Ti:sapphire laser is focused onto a GaSe or ZnTe crystal to generate THz radiation by difference-frequency mixing. After collimation by a 90° off-axis parabolic mirror PM1, the remaining generation light is blocked by a high-resistivity Si wafer whereas the THz radiation is transmitted and focused by PM2 onto the sample. After recollimating by PM3 and refocussing by PM4, the THz beam finally transmits the ZnTe crystal for detection. A 2nd Si wafer is employed to combine the THz beam with a beam of near-infrared sampling pulses such that the 2 beams propagate collinearly through ZnTe. The THz-induced ellipticity of the sampling beam is detected by using a $\lambda/4$-wave plate and a Wollaston prism. The MHz setup employs spherical mirrors instead of lenses to avoid unnecessary longitudinal and transverse chirp of the 10-fs laser pulses.

3.2.1. THz Generation

The THz radiation covering a spectrum from 1 to 3 THz is produced by difference frequency mixing in ZnTe, whereas GaSe is employed to obtain pulses covering a spectrum from about 10 to 30 THz. The $\lambda/2$-wave plate before the generation crystal adjusts the polarization of the generation beam, which is 45° with respect to the p direction in case of GaSe and 0° in case of ZnTe. The resulting THz radiation is p polarized. The GaSe crystal can be rotated about an axis parallel to the laser table to change the phase matching angle ϑ_{inc} as shown in Fig. 2.6.

Although the electric field of each laser pulse has the same envelope, the phase between the envelope and the carrier wave generally differs from shot to shot [Bra00]. Fortunately, the THz generation process does *not* depend on the absolute phase of the input pulse as emphasized in Section 2.3.1 and thus delivers the *same* THz waveform for each laser shot.

In the MHz setup, the generation beam is focused tightly to a diameter of $\approx 15\,\mu$m onto the generation crystal in order to generate as much THz radiation as possible. In the kHz setup, such tight focusing might damage the generation crystal which is thus placed before the focus.

3.2.2. THz Detection

As described in Section 2.3.1, the THz-pulse induces a birefringence in the ZnTe detection crystal via the electrooptic effect and thus makes the copropagating sampling pulse elliptically polarized. The ellipticity η is detected as follows: First, the $\lambda/4$-wave plate transforms the elliptically polarized light into linearly polarized light whose polarization plane is now rotated by a corresponding angle η. Second, a Wollaston prism spatially separates 2 beams of perpendicular linear polarization and is oriented such that the power of the 2 beams is equal when no THz field is present. Third, the light power is measured by a pair of photodiodes whose current difference is proportional to η. The THz signal

$$S(t) \propto \eta(t)$$

is scanned step-by-step by moving the t-delay stage in Fig. 3.3.

The MHz setup employs standard Si photodiodes which are fast enough to resolve the chopper modulation frequency of 9 kHz (see below).

In the kHz setup, the sampling pulse is derived from the *seed* laser instead from the amplified laser beam for the following reasons: First, this allows to shape the amplified pulses without changing the sampling pulse. Second, the seed pulses have a 12-fs duration and small shot-to-shot energy fluctuations of $\approx 10^{-3}$. Thus they are significantly shorter and more stable than the amplified pulses resulting in a better signal-to-noise ratio. Due to the much larger repetition rate of the seed laser, only 1 of ≈ 75000 sampling pulses coincides with a THz pulse. The temporal gating of precisely this sampling pulse requires fast photodiodes to resolve the 75-MHz sampling pulse train and an electronic gate which is provided by a boxcar integrator (Stanford SR250) [Rei03].

3.2.3. Computer-Controlled Data Acquisition

In both the MHz and the kHz setup, the 2 photodiodes deliver a current or voltage signal $S_0 + \Delta S + O$. Here, S_0 is due to the THz electric field when the pump-beam is off, and ΔS is caused by the pump-induced changes of the THz field. The slowly varying offset O is due to drifts in the setup which can also lead to a photodiode signal although the THz beam is blocked. The goal is to measure both THz signals S_0 and ΔS which is achieved by "marking" these signals with different modulation frequencies.

In the MHz setup, a chopper wheel chops the THz generation beam leading to a multiplication of the total THz signal with a modulation function M_1 of fundamental frequency $f_1 \approx 9\,\text{kHz}$. Another chopper in the pump beam modulates the pump-induced signal with a function M_2 centered at a frequency $f_2 \approx 70\,\text{Hz}$. The total electric signal $O + S_0 \cdot M_1 + \Delta S \cdot M_1 M_2$ after the photodiodes is fed into a lock-in amplifier (Stanford Research SR830) which is phase-locked to M_1. The lock-in amplifier acts as a spectral filter and rejects possible noise like a dc offset O outside its filter band which is much

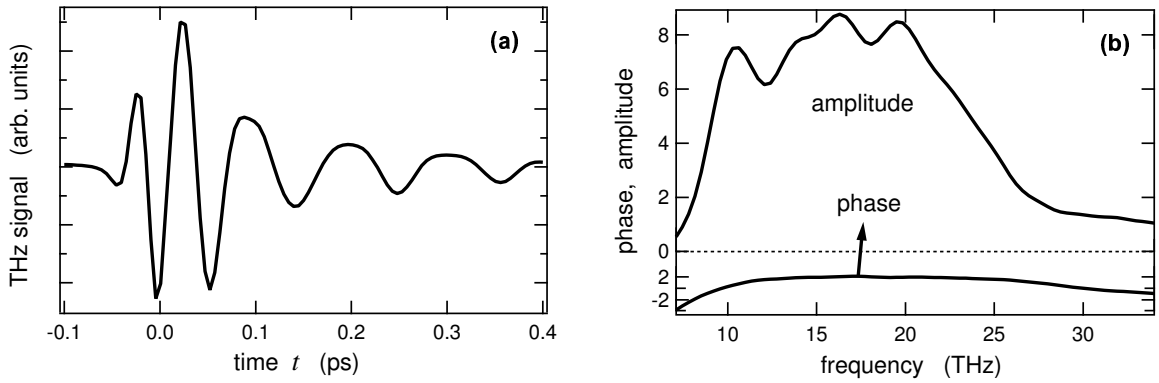

Figure 3.4.: (a) Typical THz waveform taken with the MHz setup. This waveform implies a pulse duration of about 100 fs. (b) Spectral amplitude and phase of the waveform in (a). The amplitude spectrum implies a bandwidth of about 15 THz. The spectral phase is essentially flat apart from the phase distortion below 10 THz where the refractive index of GaSe shows strong variations due to the presence of phonon resonances [Sch05].

broader than f_2; thus its output is $S_0 + \Delta S \cdot M_2$ and oscillates at a frequency f_2. Feeding the output of the 1st lock-in amplifier into a 2nd lock-in amplifier phase locked to M_2 eventually gives ΔS. The 2 lock-in amplifiers are read out by a personal computer via an IEEE-488 interface at a rate of 512 Hz. Numerical averaging yields the signals $S_0 + \Delta S/2$ and $\Delta S/2$, respectively.

In the kHz setup, a possible signal background O is greatly reduced by a circuit which consists of a delay line and a current inverter. They perform a subtraction of each current pulse from its preceding pulse. Thus, the boxcar integrator delivers the signal S_0 or $S_0+\Delta S$ depending on whether the pump beam is blocked or not. S_0 and $S_0 + \Delta S$ are obtained separately by blocking every 2nd pump pulse with a mechanical chopper. The boxcar integrator is read out shot-by-shot by a personal computer via a fast analog-to-digital conversion card (National Instruments PCI-MIO 16E4).

All data-acquisition software is written in LabVIEW (National Instruments). It also controls the electronic delay stages and features special tools to optimize the THz signal.

3.2.4. Technical Data

Figure 3.4 shows an exemplary THz waveform together with its spectral amplitude and phase. Note that the pulse has a duration of about 100 fs. The oscillations found for $t > 0.1$ ps are due to the distortion of the spectral phase at about 10 THz which originates from strong variations of the refractive index of GaSe.

Table 3.1 shows typical parameters of the two THz spectrometers. In the MHz setup, the signal-to-noise ratio is limited by the shot noise of the sampling beam. An average time of 1 s implies a filter bandwidth of 1 Hz and thus a signal-to-noise ratio of up to 10^4. With this sensitivity one can still detect pump-induced phase shifts of a 20-THz wave which

parameter	MHz setup	kHz setup
pulse repetition rate	75 MHz	1 kHz
THz peak electric field in focus	$\sim 100\,\mathrm{V\,cm^{-1}}$	$\sim 100\,\mathrm{kV\,cm^{-1}}$
THz pulse duration	≈ 100 fs	≈ 100 fs
THz spectrum	10 to 30 THz	10 to 25 THz
THz-focus diameter on sample	50 μm (intensity FWHM)	50 μm (intensity FWHM)
signal-to-noise ratio	up to $10^4\,\mathrm{Hz^{-1/2}}$	up to $10^3\,\mathrm{Hz^{-1/2}}$

Table 3.1.: Typical parameters of the two THz spectrometers.

correspond to a length of less than 1 nm. Since the path difference between the THz and sampling pulse drifts by roughly 20 nm per minute measurements of the THz waveforms have to be performed fast.

3.2.5. Sample Requirements

As the THz spectrometer probes the sample in transmission geometry, the sample has to be transparent for the THz radiation. Moreover, the pump-probe experiments require a substrate to minimize the thermal load of the sample induced by the pump pulse. Diamond is the ideal substrate material since it is transparent in the THz and visible spectral range and exhibits a good thermal conductivity. Moreover, it introduces negligible dispersion and only very small thermally induced phase shift changes in the far- and mid-infrared [Ruf00].

3.3. Work Sequence of THz Spectroscopy

The ultimate goal of every THz transmission experiment is to obtain the dielectric function ε of the sample. For this purpose, the sample response to the THz radiation has to be compared to that of a sample with known response. The typical work steps in THz spectroscopy are the following:

1. Measure the THz signal S for the sample of interest.
2. Measure the THz signal S_{ref} for a reference sample which is a sample with well-known THz response.
3. Fourier-transform $S(t)$ and $S_{\mathrm{ref}}(t)$ with respect to t and use the ratio

$$Q(\omega) = \frac{S(\omega)}{S_{\mathrm{ref}}(\omega)}$$

   to determine the dielectric function $\varepsilon(\omega)$.

We discuss 2 typical examples:

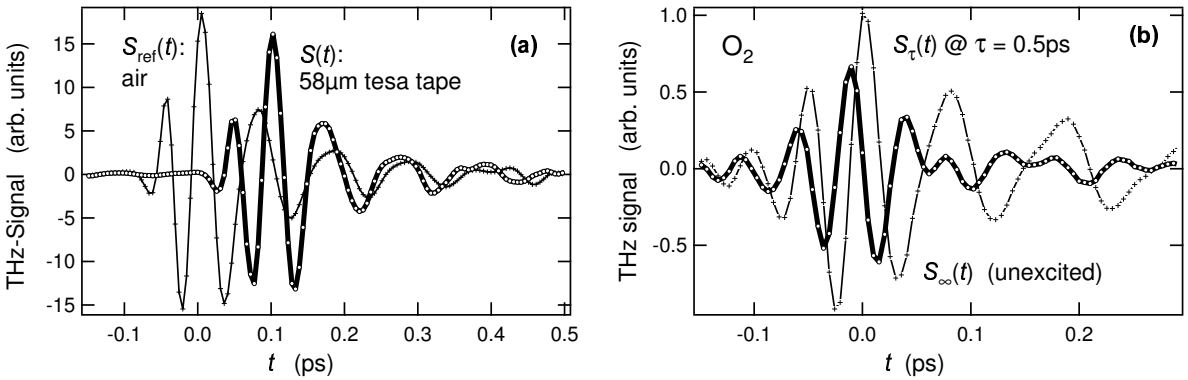

Figure 3.5.: Examples of the THz signal S taken with the sample of interest and the reference signal $S_{\mathrm{ref}}(t)$ from a sample of known response. (a) THz signal $S(t)$ after transmission of a 58 μm-thick tape (tesa kristallklar), and the reference signal $S_{\mathrm{ref}}(t)$ without the sample. The tape delays the THz arrival at the detector by about 100 fs. Apart from this delay and an overall amplitude decrease, the tape does not severely distort the shape of the THz signal. (b) THz signal $S(t) = S_{0.5\,\mathrm{ps}}(t)$ after transmission through a 20 μm-thick film of optically ionized oxygen O_2 0.5 ps after excitation. The reference signal $S_{\mathrm{ref}}(t) = S_\infty(t)$ is taken for unexcited O_2. Parts of S arrive earlier at the detector than these of S_∞ since the real part of the refractive index of the laser-induced plasma is smaller than 1.

- Figure 3.5(a) shows data of a *steady-state* measurement where S is obtained after transmission through "tesa" tape. The reference signal S_{ref} is measured without tape.

- Figure 3.5(b) shows data of a *pump-probe* experiment where $S = S_\tau$ is taken for gaseous oxygen O_2 at a fixed delay τ after ionization of the gas by an intense pump pulse. $S_{\mathrm{ref}} = S_{\tau=\infty} = S_\infty$ is obtained for the sample without, that is a long time after or before the excitation. Instead of $Q_\tau = S_\tau / S_\infty$ one often considers the pump-induced change

$$\Delta Q_\tau(\omega) = Q_\tau(\omega) - 1 = \frac{\Delta S_\tau(\omega)}{S_\infty(\omega)}.$$

As shown below, knowledge of the experimental quantity Q allows to extract the dielectric function of the sample. The division connected with the calculation of Q has important advantages:

- All spectrometer-related response functions cancel out at least for a slowly varying sample. This is especially the case for the detector response which was observed to drift slowly in the course of time due to degradation of the ZnTe crystal. Slow intensity variations of the generation and sampling pulse cancel in the same way.

- A slow temporal drift between the THz and the sampling pulse is removed since a temporal shift affects both S and S_{ref}. The resulting phase factor in ω space cancels in the division S/S_{ref}.

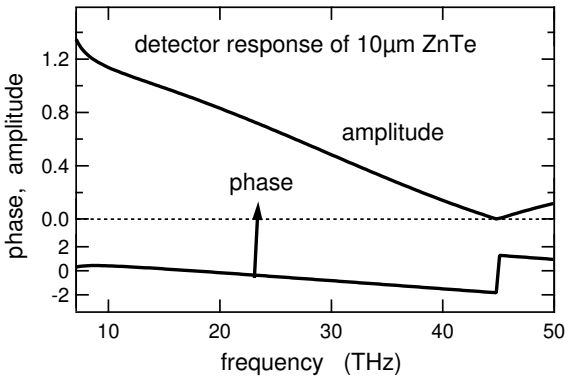

Figure 3.6.: Electrooptic detection response $R_\mathrm{d} = \eta(\omega)/E_\mathrm{ZnTe}(\omega)$ of a 10-μm thick ZnTe crystal [Lei99a]. Here, E_ZnTe is the THz electric field directly before the ZnTe crystal and η the induced ellipticity of the sampling beam. The origin of the vanishing response at 45 THz is detailed in Fig. 2.2.

3.4. Extraction of the Dielectric Function

Strictly speaking, the THz signal S measured is *not* the electric THz field E directly after the sample; it is rather the ellipticity η of the sampling pulse that is induced by the copropagating THz field within the detection crystal. Therefore, S and E are related by

$$S(\omega) = E(\omega)\, R_\mathrm{pd}(\omega)$$

where the function $R_\mathrm{pd} = R_\mathrm{p} R_\mathrm{d}$ describes the THz propagation R_p from the sample to the detector and the detection process R_d itself. The detector response R_d is detailed in Fig. 3.6.

3.4.1. Steady-State Measurements

In this case and according to Eq. (1.34), the signal measured is

$$S(\omega) = E(\omega)\, R_\mathrm{pd}(\omega) = E_\mathrm{inc}(\omega) R(\omega)\, R_\mathrm{pd}(\omega)$$

where E_inc is the field incident on the sample and R the sample response. An analog expression is obtained for the reference sample with response R_ref. Note that all spectrometer-related response functions cancel such that one is left with the desired sample response

$$R(\omega) = Q(\omega) R_\mathrm{ref}(\omega).$$

R and R_ref are related to the dielectric function ε of the sample by standard formulas such as Eq. (2.12). Inverting these relations finally yields ε which will be shown in detail for graphite in Section 4.6.3.

3.4.2. Pump-Probe Measurements

In this kind of experiment, the signal measured is a 2-dimensional mesh $\Delta S_\tau(t) = S_\tau(t) - S_\infty(t)$ where τ is the delay between pump and probe pulse. In the following we consider

the pump-induced changes $\Delta S_\tau = S_\tau - S_\infty$. In general, it is necessary to Fourier-transform the raw data with respect to both times t and τ which implies the variable changes $t \longrightarrow \omega$ and $\tau \longrightarrow \Omega$. According to Eq. (2.15), the resulting $\Delta S_\Omega(\omega)$ is related to the changed electric field $\Delta E_\Omega(\omega)$ after the sample by

$$\Delta S_\Omega(\omega) = \Delta E_\Omega(\omega)\, R_{\mathrm{pd}}(\omega) = E_{\mathrm{inc}}(\omega - \Omega)\Delta R_\Omega(\omega - \Omega)\, R_{\mathrm{pd}}(\omega),$$

where ΔR_Ω is the pump-induced change in the sample response.

The reference signal for the unexcited sample is $S_\infty = E_{\mathrm{inc}} R_\infty R_{\mathrm{pd}}$. Thus, one finally obtains

$$\Delta R_\Omega(\omega - \Omega) = R_\infty(\omega)\Delta Q_\Omega(\omega)\frac{E_{\mathrm{inc}}(\omega)}{E_{\mathrm{inc}}(\omega - \Omega)}. \tag{3.1}$$

Since the sample modulates the incident electric field by frequencies Ω, E_{inc} does not cancel any more in the last equation. It is in principle possible to reconstruct the incident electric field from the THz signal S by taking the propagation from the sample to the detector and the detector response into account [Něm02]. It turned out for all relevant data in this work, that this is not necessary: Due to the large bandwidth of the THz pulses of about 10 to 15 THz, E_{inc} has a quite flat spectrum such that the last factor in Eq. (3.1) is close to unity.

The dielectric function is obtained from ΔR_Ω, for example with the aid of Eq. (2.16), and an inverse Fourier transformation with respect to Ω yields its instantaneous spectral shape $\Delta\varepsilon_\tau$ at time τ after sample excitation. This procedure will be shown in Section 4.6.3 for graphite in detail.